



HAL
open science

Humanoids'feet: state of the art & future directions

Irene Frizza, Ko Ayusawa, Andrea Cherubini, Hiroshi Kaminaga, Philippe Fraise, Gentiane Venture

► **To cite this version:**

Irene Frizza, Ko Ayusawa, Andrea Cherubini, Hiroshi Kaminaga, Philippe Fraise, et al.. Humanoids'feet: state of the art & future directions. *International Journal of Humanoid Robotics*, 2022, 19 (01), pp.2250001. 10.1142/S0219843622500013 . hal-03534274

HAL Id: hal-03534274

<https://hal.science/hal-03534274v1>

Submitted on 19 Jan 2022

HAL is a multi-disciplinary open access archive for the deposit and dissemination of scientific research documents, whether they are published or not. The documents may come from teaching and research institutions in France or abroad, or from public or private research centers.

L'archive ouverte pluridisciplinaire **HAL**, est destinée au dépôt et à la diffusion de documents scientifiques de niveau recherche, publiés ou non, émanant des établissements d'enseignement et de recherche français ou étrangers, des laboratoires publics ou privés.

HUMANOID'S FEET: STATE OF THE ART & FUTURE DIRECTIONS

Irene Frizza^{1,2}, Ko Ayusawa¹, Andrea Cherubini², Hiroshi Kaminaga¹, Philippe Fraisse²,
Gentiane Venture^{1,3}

¹ *CNRS-AIST JRL (Joint Robotics Laboratory), UMI3218/RL, Tsukuba, Ibaraki, Japan.*

² *LIRMM, Université de Montpellier, CNRS Montpellier, France.*

³ *Tokyo University of Agriculture and Technology, Japan.*

Corresponding author: venture@cc.tuat.ac.jp

Received Day Month Year

Revised Day Month Year

Accepted Day Month Year

Robotic feet play a fundamental role in the walking performance of a biped robot. Feet are essential to maintain dynamic stability and to propel the body during walking. They may ensure stability on uneven terrains. Yet, complex feet are seldom used on humanoids. This paper surveys 36 types of robotic feet we found in the literature. We classified them according to strategy, capabilities, structure, number of degrees of freedom, actuation method of ankle and foot, type of actuator, sensorization and type of control. Subsequently, we analyzed the dynamic and static models of flexible feet. We discussed considerations on foot dynamics or kinematics in the robot's whole body control system. We analyzed both active joints control for feet including actuated joints, and control for feet with elastic elements (for example, a rubber layer in the sole). Finally, we present some limitations of robotic feet and possible future developments.

Keywords: robotic feet, biped locomotion, humanoid robots.

1. Introduction

Locomotion is an important topic in humanoid robotics research. More than 20 years ago, researchers already started to study strategies on how legged robots can move over rough terrain by adjusting the step length and the distance traveled between successive steps for example [1,2]. Yet, even common functions of the human such as walking, running or dancing, are difficult to perform by a humanoid. The human foot has been an inspiration for the design of humanoid feet. The human foot can adapt to many different conditions, such as the presence of obstacles and rough terrain, act as shock absorber and propeller, and help maintaining the balance.

This paper proposes a survey and classification of the state of the art of humanoid feet and future directions for the development of new devices. Feet are classified according the six following features: (1) goal of the foot, (2) capabilities related to the legs performance, (3) design of the foot structure, (4) number of degrees of freedom, (5) actuation method, (6) type of actuation, (7) sensorization,

2 I. Frizza, K. Ayusawa, A. Cherubini, H. Kaminaga, P. Fraise, G. Venture

(8) integration of the foot in the robot model and (9) in the control system. To identify the papers to be included in this state of the art, we used Google Scholar. As scientific databases, we used IEEE Xplore, ResearchGate, Springer and Elsevier. The papers were chosen based on the search keywords: “humanoid feet”, “robotic feet”, “humanoid robot walking”, “bipedal locomotion”. A paper was included in this survey if it provided complete information on the structure (and possibly sensors and actuation) of the robotic foot and if it presented real robotic feet (not just simulated). We included only feet used for biped robot walking. In total 36 feet in 60 papers were retained. They are presented in Table 1.

2. Anatomy of the human foot

The human feet are often used as inspiration of humanoids feet. Let us briefly introduce the human foot structure and some terminology [3]. The foot anatomy consists of 26 bones, 33 joints and numerous muscles, tendons, ligaments, nerves and soft tissues. As shown in Fig. 1, the foot is divided into three anatomical sections called hindfoot, midfoot, and forefoot, attached to the leg by the ankle joint.

The *hindfoot* connects the midfoot to the ankle at the transverse tarsal joint and consists of the talus bone (in the ankle) and the calcaneous bone (in the heel). The calcaneous bone and the talus bone are respectively the largest bones in the foot. The calcaneous bears large loads during weight bearing and joins the talus bone at the subtalar joint, enabling the foot to rotate at the ankle. The *midfoot* connects to the forefoot at the metatarsal joints and contains five tarsal bones. Ligaments and muscles make the connection from the forefoot to the hindfoot through the midfoot. The main ligament is the plantar fascia. The midfoot transmits and attenuates forces and allows the foot to accommodate to variable ground surfaces. It forms the arches of the foot and acts as a shock-absorber, when walking or running. The arches are supported and controlled by a combination of bones, muscular and ligamentous



Fig. 1. Anatomic representation of the human foot and ankle, showing the major bones constituting the hindfoot, the midfoot and the forefoot, and the plantar fascia ligament linking the hindfoot to the forefoot. (<https://www.coastlineortho.com/>)

structures making the foot efficient for locomotion [4]. The *forefoot* consists of the toe bones (phalanges) and metatarsal bones. Each toe has three phalange bones and two joints, while the big toe contains two phalange bones (proximal and distal), two joints, and two tiny, round bones (sesamoid bones) which enable the pitch movement of the toe. The metatarsal heads act as a lever for propulsion in the terminal position and they adapt to the change of the gravitational axes, for the stability. The *ankle joint* is made of three bones attached by muscles, tendons and ligaments, which connect the foot to the leg. In the lower part of the leg there are two bones: the tibia (shin) and the fibula. These bones connect to the ankle joint, allowing dorsiflexion (pulling the foot upwards towards the lower leg) and plantarflexion (pulling the foot downwards away from the lower leg). The tibia and the fibula are coupled to ankle motion by the tibial rotation, which is coupled to hindfoot, connected to fibular translation and rotation in all cardinal planes.

3. Classification of Robotic Feet

This section presents the surveyed 36 robotic feet and compares them according to six significant features we identified: overall goal, capabilities, structure, number of degree of freedom (DoF), actuation for each ankle and each foot, type of actuator, sensorization and type of feedback when control is applied. Each of these features is presented below and all feet are summarized in Table 1.

3.1. Goal

The *goal* defines the main expected functional purpose of the foot: i.e. shock absorption, adaptability to uneven terrain, energy storage, stability... and the idea behind the foot structure, i.e. which inspiration has been followed to design the foot.

3.2. Capabilities

Capabilities refers to effect of the legs. Some classified robotic feet have been developed together with the leg to perform different types of actions: standing, walking, stair climbing, running or jumping. Some of the analyzed structures are not yet tested on humanoid robots and we are not able to analyze the legs performance, so we could not mark their capabilities in the table.

3.3. Structure

Structure refers to the physical structure of the foot. Most humanoids adopt flat feet consisting of a unique rigid segment [5–30] or of two rigid segments joined by a revolute joint [31–40, 42–51]. One humanoid robot adopts a different solution with a unique rigid segment with a wheel on the foot [41]. Fig. 2 shows the feet of these categories. Finally, few robotic feet are designed with a more complex structure [52–59], or with soft structures [60–64]. Fig. 3 shows these feet.

Table 1. Classification of types of robotic feet ordered by complexity of Structure, DoF of the foot and Actuation

| [Reference] Robot or foot name (Figure) | Goal | | | | Capabilities | | | | | | | Structure | DoF, Actuation ¹ | Type of Actuation | Sensor ² Model | Type of control (Loop) | | | |
|---|-------------------|----------------|----------------------|----------------------------------|---------------------------------|----------------|---------------------------|--|---------------------------------------|----------------------|----------|-----------|-----------------------------|-------------------|---------------------------|------------------------|---------|----------------|---------|
| | Impact Absorption | Stable walking | Prevent tipping over | Move in inhospitable environment | Adaptability on uneven terrains | Energy storage | Lightness and compactness | Operate freely in the human living space | Extension capabilities with toe joint | Imitate human motion | Standing | | | | | | Walking | Stair Climbing | Running |
| [5, 6] WL-12RVII 2(a) | ✓ | ✓ | | | | | | | | | ✓ | ✓ | ✓ | ✓ | 0 | AC Servomotor | Yes | Yes | Closed |
| [7, 8] CASSIE 2(b) | | ✓ | | | ✓ | | | | | | | | | | 0 | Brushless DC | Yes | Yes | Closed |
| [9] WABIAN-2R | | | | | | | | | | | | | | | 0 | Brushless DC | Yes | No | — |
| (unique segment) 2(c) | ✓ | ✓ | | | | | | | | | ✓ | ✓ | ✓ | ✓ | 2 A | Brushless DC | Yes | Yes | — |
| [10-12] BHR-2 2(d) | ✓ | ✓ | | | | | | | | | ✓ | ✓ | ✓ | ✓ | 2 A | Brushless DC | Yes | Yes | — |
| [13, 14] HRP-2 2(e) | ✓ | ✓ | ✓ | | | | | | | | ✓ | ✓ | ✓ | ✓ | 0 | Brushless DC | Yes | Yes | — |
| [15] WALK-MAN 2(f) | ✓ | ✓ | | | | | | | | | ✓ | ✓ | ✓ | ✓ | 2 A | Brushless DC | Yes | Yes | — |
| [16] P2 2(g) | ✓ | ✓ | | | | | | | | | ✓ | ✓ | ✓ | ✓ | 2 A | Brushless DC | Yes | Yes | — |
| [17, 18] HRP-4 2(h) | ✓ | ✓ | | | | | | | | | ✓ | ✓ | ✓ | ✓ | 0 | Brushless DC | Yes | No | — |
| [19, 20] KHR-3 2(i) | ✓ | ✓ | | | | | | | | | ✓ | ✓ | ✓ | ✓ | 2 A | Brushless DC | Yes | No | — |
| [21] PYRENE (TALOS) 2(j) | | ✓ | | | | | | | | | ✓ | ✓ | ✓ | ✓ | 0 | Brushless DC | Yes | No | — |
| [22] JAXON 2(k) | | ✓ | | | | | | | | | ✓ | ✓ | ✓ | ✓ | 0 | Brushless DC | Yes | No | — |
| [23, 24] VALKYRIE 2(l) | | ✓ | | | | | | | | | ✓ | ✓ | ✓ | ✓ | 0 | SEA | Yes | No | — |
| [25-28] NAO 2(m) | | ✓ | | | | | | | | | ✓ | ✓ | ✓ | ✓ | 2 A | Brushless DC | Yes | No | — |
| [29, 30] ASIMO 2(n) | | ✓ | | | | | | | | | ✓ | ✓ | ✓ | ✓ | 0 | Brushless DC | Yes | No | — |
| [31] Ken 2(o) | | ✓ | | | | | | | | | ✓ | ✓ | ✓ | ✓ | 1 A | Brushless DC | Yes | No | — |
| [32, 33] ROBIAN 2(p) | | ✓ | | | | | | | | | ✓ | ✓ | ✓ | ✓ | 1 P | Brushless DC | Yes | Yes | — |
| [34] iCub 2(q) | | ✓ | | | | | | | | | ✓ | ✓ | ✓ | ✓ | 2 A | Brushless DC | Yes | Yes | — |
| [35] WABIAN-2R | | | | | | | | | | | ✓ | ✓ | ✓ | ✓ | 2 A | Brushless DC | Yes | Yes | — |
| (two-segments) 2(r) | | | | | | | | | | | ✓ | ✓ | ✓ | ✓ | 2 A | Brushless DC | Yes | Yes | — |
| [36-40] 2(s) | | | | | | | | | | | ✓ | ✓ | ✓ | ✓ | 2 A | Brushless DC | Yes | Yes | — |
| [41] DRG-HUBO+ 2(t) | | | | | | | | | | | ✓ | ✓ | ✓ | ✓ | 1 P | Brushless DC | Yes | Yes | Closed |
| [42, 43] H6 2(u) | | | | | | | | | | | ✓ | ✓ | ✓ | ✓ | 2 A | Brushless DC | Yes | Yes | Closed |
| [44] UT-μ2 2(v) | | | | | | | | | | | ✓ | ✓ | ✓ | ✓ | 2 A | Brushless DC | Yes | Yes | Closed |
| [45] BIPMAN 2(w) | | | | | | | | | | | ✓ | ✓ | ✓ | ✓ | 1 A | Pneumatic actuator | Yes | No | Closed |
| [46, 47] PNEUMAT-BH 2(x) | | | | | | | | | | | ✓ | ✓ | ✓ | ✓ | 2 A | Pneumatic actuator | Yes | No | Closed |
| [48] HRP-4C 2(y) | | ✓ | | | | | | | | | ✓ | ✓ | ✓ | ✓ | 1 A | Brushless DC | Yes | Yes | Closed |
| [49] ARMAR-4 2(z) | | | | | | | | | | | ✓ | ✓ | ✓ | ✓ | 2 A | Brushless DC | Yes | Yes | Closed |
| [50, 51] LOLA 2(aa) | | | | | | | | | | | ✓ | ✓ | ✓ | ✓ | 1 A | Brushless DC | Yes | Yes | Closed |
| [52] PNEUMAT-BB-3(a) | | ✓ | | | | | | | | | ✓ | ✓ | ✓ | ✓ | 2 A | Pneumatic actuator | Yes | No | Open |
| [53-55] WABIAN-2R | | | | | | | | | | | ✓ | ✓ | ✓ | ✓ | 2 A | Brushless DC | Yes | No | Open |
| (multi-joint) 3(b) | | | | | | | | | | | ✓ | ✓ | ✓ | ✓ | 2 A | Brushless DC | Yes | No | — |
| [56] Seo et al. 3(c) | | | | | | | | | | | ✓ | ✓ | ✓ | ✓ | 3 P | — | No | No | — |
| [57] Yalananchili et al. 3(d) | | | | | | | | | | | ✓ | ✓ | ✓ | ✓ | 0* | — | No | No | — |
| [58] Yoon et al. 3(e) | | | | | | | | | | | ✓ | ✓ | ✓ | ✓ | 4 A | Pneumatic actuator | No | No | — |
| [59] Kuehn et al. 3(f) | | | | | | | | | | | ✓ | ✓ | ✓ | ✓ | 4 A | Brushless DC | Yes | Yes | — |
| [60-62] Kengoro 3(g) | | | | | | | | | | | ✓ | ✓ | ✓ | ✓ | 16A | Brushless DC | Yes | Yes | Closed |
| [63] Davis et al. 3(h) | | ✓ | | | | | | | | | ✓ | ✓ | ✓ | ✓ | 20A | Brushless DC | Yes | Yes | Closed |
| [64] SoftFoot 3(i) | | | | | | | | | | | ✓ | ✓ | ✓ | ✓ | 56P | — | No | No | — |

¹ The number represents the number of DoFs, the letter A means "active" and the letter P means "passive" for the actuation type. See Table 2 for details about how many and which DoFs are actuated

² See Table 3 for details about sensors

* The foot is composed only of a plantar fascia or platform

3.4. Degrees of Freedom and Actuation

Degrees of Freedom

Each robotic foot can be classified according to the number of degrees of freedom. Table 2 shows the number of DoF of the ankle and of the foot in the surveyed works.

Actuation

As Table 1 shows, we have also classified robotic feet based on power source method (active or passive). An active actuation relies on an external source of power (such as a battery) to operate an actuator providing force or torque. On the other hand, a passive foot produces forces from the action of springs or damping elements, which can change the feet attitude when it comes in contact with the ground. Also in this section, we will consider both ankle and foot.

3.5. Sensors

Most of the robotic feet are equipped with sensors. These include measurements on the foot or ankle. Generally, the sensors measure the ground reaction force (GRF), the displacement of the foot, the tilt angle, the detection of contact between the foot and the ground and the pressure. Table 3 show which sensors are used to measure these quantities, along with their components.

3.6. Models

The development of the foot model represents one of the main problems in bipedal walking [65], since the structure of the foot is complex and the modeling of contact is not trivial. However, the dynamic model of humanoids is important to estimate the response of the robot and its interaction with the ground during operations when conducting simulations, and when using advanced control schemes. Table 1 also shows for which robots models of the foot are available, as well as some walking models.

3.7. Control

We finally classified robotic feet based on the type of control (closed loop or open loop). However, as Table 1 shows, there are few control systems which include foot dynamics or kinematics. These works are mainly divided into two categories: foot which has some actuated joints (often, the actuated joint is the toe pitch) and foot for which the structure is completely flat, but includes elastic elements which can be added to the robot dynamic model.

3.8. Survey and discussion

3.8.1. Goal

Most robotic feet aim at reproducing the functions of the human foot and at performing human-like motions. In ROBIAN [32, 33], the flexible feet simulate the human locomotion with a parallel mechanism at the ankle and one passive joint between the heel and toe. Ogura *et al.* describes WABIAN-2R as capable of human-like walk with stretched knees, heel contact and toe-off motions, using a foot mechanism with a passive toe joint [35]. The feet of HRP-4C [48], of UT- μ 2 [44], of ARMAR-4 [49], and of BIPMAN [45] were developed with an active toe joint to realize human-like walking motions. SoftFoot [64], Kengoro's foot [60–62], Yalamanchili *et al.* structure [57] and Yoon *et al.* foot [58] aim at reproducing the flexibility of the human foot by using multiple joints. The second most common goal of the feet are to allow stability and adaptability when walking on uneven terrains [5–9, 13, 17, 18, 46, 47]. Kang *et al.* developed a mechanism to detect ground surface to stabilize the walk of Wabian-2R [9]. Several types of foot structure, sometimes with many joints, to ensure that the foot adapts to the ground in the presence of obstacles have also been proposed [56, 59, 63, 64]. To achieve environmental contact actions or the balancing on a rough terrain, Asano *et al.* added flexibility to the foot structure of Kengoro [60–62], while Kanehira *et al.* proposed to use visco-elastic elements [14]. Another common goal is the absorption of the foot impact on the ground. Some feet are designed to absorb the shock with the ground [16] and also to store and release energy during this phase [19, 20, 52, 63]. To do so, some structures include layers of visco-elastic material to absorb impact with the ground. For example, in HRP-2 [13] the foot structure consists in a combination of a rubber sole and bushes under the force sensor. In BHR-2 [10–12], the authors adopt rubber bushes and rubber pads for absorbing landing impacts when the humanoid robot is moving. In WL-12RVII [5, 6] the foot is equipped with an absorption mechanism that uses cushioning materials. Enabling mobility in inhospitable environment is the main goal of robots such as WALK-MAN [15], PYRENE [21], JAXON [22], VALKYRIE [23, 24], DRC-HUBO+ [41], LOLA [50, 51] and HRP-2 [13, 14]. Some robotic feet designs aim at extending walking capabilities with the insertion of the toe joint. With this joint, H6 [42, 43] can move forward with its knees in contact with the ground. Eldirdiry *et al.* provide a robotic foot with a passive joint and try to avoid foot drop [36–40]. Takahashi *et al.* proposed an active joint in the foot for the first time and implemented it in the robot Ken [31]. With these feet, the robot could walk also when contact between the foot sole and the ground was reduced to a contact point. The robot ASIMO feet designed to enable the robot to go up and down stairs, walk on an uneven ground and operate freely in the human living space [29, 30]. Finally, the robot NAO [25–28] foot was designed to be lightweight with two rotary joints in the ankle-foot structure, to make a unique joint module.



Fig. 2. Robotic feet with a one segment structure, with one segment with a wheel or with two segments structure (a) WL-12RVII [5, 6], (b) CASSIE [7, 8], (c) WABIAN-2R (unique-segment mechanism) [9], (d) BHR-2 [10–12], (e) HRP-2 [13, 14], (f) WALK-MAN [15], (g) P2 [16], (h) HRP-4 [17, 18], (i) KHR-3 [19, 20], (j) PYRENE (TALOS) [21], (k) JAXON [22], (l) VALKYRE [23, 24], (m) NAO [25–28], (n) ASIMO [29, 30], (o) Ken [31], (p) ROBIAN [32, 33], (q) iCub [34], (r) WABIAN-2R (two-segments mechanism) [35], (s) [36–40], (t) DRC-HUBO+ [41], (u) H6 [42, 43], (v) UT- μ 2 [44], (w) BIPMAN [45], (x) PNEUMAT-BH [46, 47], (y) HRP-4C [48], (z) ARMAR-4 [49], (aa), LOLA [50, 51].

3.8.2. Capabilities

Most robotic feet and legs have been designed together to give the humanoid the ability to stand and walk. Only Kengoro [60–62] is not able to walk but has the abilities to stand.

The other classified humanoids are able to walk, at different speeds: for example WABIAN-2R (two-segments) [35] can walk up to 0.27 m/s, KHR-3 [19, 20] up to 0.35 m/s, BHR-2 [10–12] can reach 0.56 m/s, HRP-2 [13, 14] can reach 0.69 m/s and NAO [25–28] can arrive at walking speed of about 0.17 m/s. For LOLA [50, 51], researchers aim to realize fast walking and they reach the impressive maximum walking speed of 0.94 m/s. Some robots are able to walk straight and sideways, turn and walk on an inclined plane: for example WABIAN-2R (unique segment) [9]

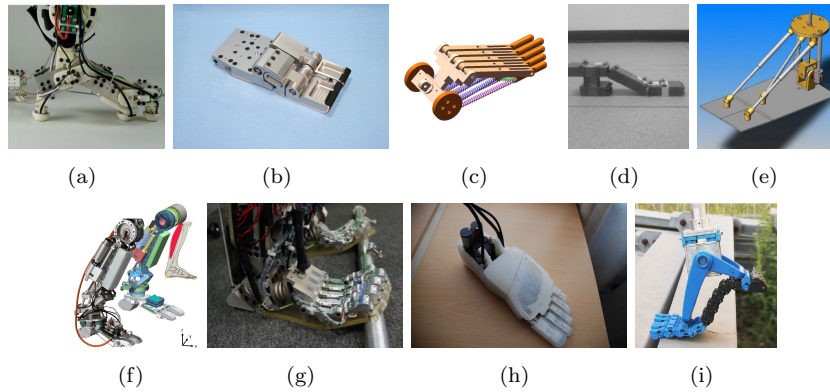
8 *I. Frizza, K. Ayusawa, A. Cherubini, H. Kaminaga, P. Fraise, G. Venture*

Fig. 3. Robotic feet with multiple segments structure or with soft structure (a) PNEUMAT-BB [52], (b) WABIAN-2R (multi-joint mechanism) [53–55], (c) [56], (d) [57], (e) [58], (f) [59], (g) KENGO [60–62], (h) [63], (i) SoftFoot [64].

is able to walk on an inclined plane of up to 7 degrees and with a maximum height of 15mm.

Many humanoids are also able to climb stairs. In bipedal locomotion, in fact, the ability to walk up stairs is important to be able to explore new industrial environments and walk on multi-contact scenarios. For example, BHR-2 [10–12] can step upstairs up to 0.15m. P2 [16] is able to walk up and down the staircase of typical buildings (0.2m height and 0.22m depth of each step) at a normal human speed. HRP-4 [17, 18] performed dynamic stair climbing in an industrial environment over 0.185m steps and P6 reached 0.25m height step climbing. There are few humanoid robots able to run. In fact, running requires the ability to maintain balance while switching positions. Researchers studied symmetric patterns of body and leg motion, to simplify running control [66]. The legs ability of CASSIE [7, 10] is very advanced: the robot successfully completed a 5000m outdoor run in 53 minutes. The latest version of ASIMO [29, 30] can walk, run, run backward, hop on one leg or on two legs continuously. In particular, it can run at a speed of 1.67 m/s. HUBO 2 [67] can run at a maximum speed of 1 m/s. The new JAXON3-P [68], with physical joint compliance by series elastic actuators, is capable of high jumping motions (0.3m height) and of stabilizing its own balance during whole-body motions. Finally, Atlas [69] is one of the most athletic humanoid robots in the world. Its advanced control system enables highly diverse and agile locomotion. Its capabilities are very impressive: it is able not only to perform a simple run and to jump, but also to perform a running jump into a platform, jumps with both feet, running along a balance beam, jumping and doing flips etc [70]. It has completely flat feet, but despite this simple structure, it has enormous walking skills on uneven terrains. However, Atlas was not included in the classification table due to the lack of published details regarding its feet: structure, sensorization, actuation, model.

3.8.3. Structure

The feet of most humanoids are made up of a single rigid segment. This simplest structure increases the risk of falling during the walking. Without compliance in the ankle, the foot is unable to adapt to the ground, causing loss of balance. To limit this problem, some humanoids adopt layers of visco-elastic material under the sole of the foot [71]. For example, in the WAF-3 foot mechanism installed on the biped walking robot WL-12RVII [6], there is a 20 mm layer of silicon foam and two layers of polyurethane rubber. Similarly, the feet of HRP-2 [13], BHR-2 [10] and P2 [16], include rubber bushes and rubber pads to avoid slipping and to increase adaptation to the ground. In particular, in P2's foot [16], rubber bushes are inserted in a guide to give elasticity in the vertical direction. In BHR-2 [10], four pieces of grommet are attached to the four corners of the foot bottom, to prevent slipping and reduce the impact shock between the foot sole and the ground. The iCub designers addressed the problem of energy dissipation during the foot impact with the ground [72]: Choi *et al.* developed a viscous air damping sole to reduce the impact on the ground forces at the foot while walking and landing. The sole is based on three air containers which are at the tip and heel of the foot. The results of the tests with this new mechanism show the reduction not only of the impact force, but also of the joint torque. The structure of the foot of WALK-MAN is singular [15]: it is composed of four layers: two metal layers, a rubber layer in the middle to reduce the peak force during impact, and another rubber layer under the bottom metal plate to increase the grip between the foot and the ground. The special feature of the DRC-HUBO+ biped [41] is that, despite having a completely flat foot, it includes a passive caster in each foot, to make the robot pivot in tight spaces. The wheel is attached to the side of the corresponding foot. In fact, the robot presents a dual-mode strategy to extend mobility by including both walking and wheel mode. This technique enables the biped to perform various actions, including traversing uneven terrain by walking, and moving across smooth terrain more quickly and stably with the wheel mode.

Some robot feet have a revolute joint that connects two rigid segments. This does not allow complete adaptability to the different types of terrain but a greater balance in the presence of obstacles, compared to the unique segment structure. This structure may allow a more human-like walking [73]. In fact, the realization of single toe support makes walking more human-like. Some of these robotic feet consist of two rigid rectangular parts connected by a passive joint, which allows the pitch toe rotation [31–40]. The front rectangular part represents the toes following human-like inspiration, to address stability reproducing heel-contact and toe-off motion during walk. In particular, in iCub [34] the toe phalange is loaded by two torsional springs. This feature is created to take longer strides than humanoids with flat feet. As shown in Table 1, HRP-2 has a completely flat foot structure. However, simulation studies have provided an additional foot joint, the toe joint. In HRP-2TJ [74], this new joint increases the walking speed by increasing the step length.

10 *I. Frizza, K. Ayusawa, A. Cherubini, H. Kaminaga, P. Fraise, G. Venture*

Table 2. Actuation of Robotic feet: number of DoFs for both ankle and foot. For the foot, the number of active DoFs is stated in parentheses. We only consider robots for which at least one DoF is active (in either the ankle or foot).

| | FOOT DoF | | | | | | | | |
|----------------|---|---|---|------------------------------|------|--|-----------------------------|--------|--|
| | 0 | 1(0) | 1(1) Toe Pitch | 2(2) Midfoot, Forefoot | 3(0) | 4(2) Toe Pitch, Toe Roll | 16(1) Toe Pitch | 20(7)* | |
| 0 | | | | | | | | [63] | |
| 1 ^A | [5, 6] WL-12RVII [7, 8] CASSIE | [31] Ken | | | | | | | |
| ANKLE DoF | [9] WABIAN-2R [10–12] BHR-2 [13, 14] HRP-2 [15] WALK-MAN [16] P2 [17, 18] HRP-4 [19, 20] KHR-3 [21] PYRENE [22] JAXON [23, 24] VALKYRIE [25–28] NAO [29, 30] ASIMO | [32, 33] ROBIAN [34] iCub [35] [36–40] [41]DRC- HUBO+ | [42, 43] H6 [44] UT- μ 2 [45] BIPMAN [46, 47] PNEUMAT-BH [48] HRP-4C [49] ARMAR-4 [50, 51] LOLA | [52] PNEUMAT- BB | | [53–55] WABIAN-2R (multi-joint mechanism) | [58] [59] | | |
| | 2 ^A | | | | | | | | |
| | 3 ^A | | | | | | [60– 62] KEN- GORO | | |

^A All the degrees of freedom of the ankle are active. When there is 1 DoF it is the pitch, 2 are pitch and roll, joint with 3 DoFs is a spherical joint.

* The seven active DoFs in [63] are: 5 in the forefoot, 1 in the midfoot and 1 in the hindfoot.

In HRP-2LR [75], there are two torsion springs in parallel for each foot with the aim of accumulating and releasing energy during running.

Several humanoids are equipped with an active toe joint [42–51]. We can find different orientations of the joint axis. For example, in H6 [42, 43], it is placed at the center of the toe link in the forward direction to generate bi-directional torque, whereas the PNEUMAT-BH foot [46] has an oblique mid-foot joint with an axis tilted in three dimensions, which imitates the human transverse tarsal joint. The particular structure of the miniature humanoid robot UT- μ 2 [44] includes a toe joint mechanism using a parallel four-bar linkage. The key of the design using parallelogram structure is that it enables rotation of the foot around the toe base joint with pure rotation, without any slippage, which enables smooth toe-off motion.

Some robotic feet are more complex and articulated, with three, four or five segments. The Pneumat series increased the number of foot joints in PNEUMAT-BB [52], whose foot consist of three links and two joints to connect hindfoot, midfoot and forefoot. WABIAN-2R's multi-joint foot [53] and the biomimetic foot mechanism of Seo *et al.* [56] include three passive joints. In particular, Seo *et al.* structure [56] is highly articulated: it is composed of five rigid toes, five rigid metatarsal structures, the rigid heel and fifteen springs imitating the human foot muscles and tendons. These elements are connected to each other to create the rotational motion of the mid-foot and the pitch movement of the toes, to obtain a three DoF foot. Finally, five rigid segments make up three types of robotic feet [57–59]. The structure is either more articulated, to imitate the structure of the human foot [57, 58] or to improve

the adaptability to the ground [59]. In Yalamanchili *et al.* [57], the five segments connected by rotational joints represent the human bones: tibia, talus, metatarsus, heel and phalanges. The Yoon *et al.* foot [58] includes three rigid platforms: one front-left, one front-right and a rear platform. Each front platform is attached to the ankle by a limb, while the rear platform is attached to the ankle by two limbs. To improve the adaptability to the ground, Kuhen *et al.* [59] installed a rear damping mechanism between the ankle and the foot and a rubber sole.

Finally, three of the surveyed robotics feet are soft [60–64]. Their structures are more complex than the above ones, with five fingers and many more joints. In the humanoid Kengoro [60–62] there are two rotational joints in each finger and two spring joints (3DoFs each) in the backward and frontal arches. In Davis *et al.* foot [63], the authors mimic the phalanges and metatarsal joints in each finger. SoftFoot [64] has the most complex structure of all robotic feet found in our survey. The structure consists of a longitudinal arch, a backward arch, five chains each composed of ten phalanxes forming the plantar fascia, and a rigid part on the back side (heel). Each phalanx is connected to the next one through a rotoidal joint, while the sole is connected with the two arches through revolute joints. Furthermore, all of these robotic feet include visco-elastic elements, to allow greater adaptability to various terrains. In Kengoro [60–62], the plantar fascia, which connects the heel to the base of the fingers, is composed of urethane rubber. Davis *et al.* foot [63] is covered with an elastic material, similar to human skin. Finally, in the sole of SoftFoot [64], each phalanx is connected to the others through two elastic bands and a tendon, which crosses the flexible structure to improve the distribution of forces. To provide additional elasticity to the structure, five springs are positioned along the longitudinal part, to connect the backward arch with each chain and to give an elastic connection to each mechanism.

Most robotic feet are designed with a zero DoF plate to simplify problems on whole body control and motion generation. However, this rigid structure is not good for walking on non-flat ground, as it increases the risk of falling. To limit this problem, most robots adopt a simple solution in which layers of elastic material are inserted under the sole, to increase friction and use compression supports. In most cases though, the foot is still too rigid to walk on uneven terrain. Feet with several DOFs, usually a sort of toes, are primarily designed to allow for toe off for human-like walking, more complex structures reduce the risk of falling by increasing the balance on uneven ground compared to the previous structure. Adding flexibility to the foot structure improves balancing and walking performances on rough terrain, energy efficiency and shock absorption. The structure of these feet is divided into various segments connected by joints, sometimes with elastic elements such as springs and tendons. However, these structures with multi-DoF are marginal in number compared to the simplest feet. Simulation study of HRP-2 shock-absorbing mechanism [76] concluded that the absence of compliance induces strong instantaneous perturbations when each foot touches the ground. Yet, outside these phases

of impact, the compliant sole preserves a behavior close to that of rigid soles. When the compliance of the sole is increased, the peaks of the waist acceleration during walking are reduced but the waist inclination in the standing phase also increases. Compliance and deformation by adding DoF may be beneficial for handling various terrains, But is showed that increasing softness can reduce stability in balancing performance [76–78], the robot body may be subject to oscillations with the multi-DoF feet during the standing phase. Robots with flexible feet are more likely to fall. [77], also emphasized the need for an adequate model of the foot compliance. To account for this, robotic feet should feature variable stiffness, with compliance changing to obtain good performance, both during the impact phase, and during the rest of the stance phase. Choi *et al.* [79] introduced such variable compliant humanoid foot design using a leaf spring and rubber balls in series. This promising approach of variable compliance feet is still very scarce in the literature.

3.8.4. *DOF & Actuation*

Most of the surveyed feet are coupled with an ankle joint. A few feet are designed with only a plantar fascia or a platform [56, 57, 63, 64]. The ankle of most humanoids has two DoF and allows the pitch and roll rotations of the joint [9–30, 32–55, 58, 59]. In WL-12RVII [5, 6], Ken [31] and CASSIE [7, 8], the ankle allows only the pitch movement and in Kengoro [60–62] the ankle joint is a spherical joint. Only DRC-HUBO+ [41], with its passive wheel positioned on the foot, has a translational degree of freedom to the foot. Some feet however have been developed with more DoFs. Table 2 shows two structures with three DoFs [53–56], three structures with four DoFs [57–59] and three structures which stand out among the others with more than 15 DoF. There are 16 DoFs in the foot of Kengoro, 10 of them in the five fingers, 3 in the subtalar joint in the frontal arch of the foot and 3 in the transverse tarsal joint in the backward arch [60–62]. The foot structure of Davis *et al.* [63] has 20 DoFs: the joints in the forefoot allow the majority of the movements. Finally, the SoftFoot structure [64] has 56 DoFs. The structure consists in five chains of ten phalanxes each. Each chain is attached to the rigid heel by another joint. This structure gives the foot a vast mobility and great adaptation to uneven terrains. When the foot structure does not include joints, only the ankle is actuated [5–30]. Most of the articulated feet are equipped with passive internal joints [31–41, 53–55]. However, some robotic feet have active joints: motors or other kinds of actuators like artificial muscles can independently move parts of the foot [42–52, 58–63]. In Table 1, feet are classified also according to the type of actuation implemented in the ankle or foot. Table 2 summarizes how many and which DoFs are actuated for both ankle and foot. For the foot, the number of active DoFs is stated in parentheses. We only consider robots for which at least one DoF is active (either in the ankle or foot). As Table 2 shows, in most humanoids, motors provide ankle actuation to change the foot orientation [5–41].

Brushless DC Motors: they equipped most the ankle and the foot’s internal

joints of robotics feet [7,8,49–51,59–62]. In ARMAR-4 [49], the motors are controlled by servo drives in the ankle and by a custom motor control board in the toe. In LOLA [50,51] the joint of the toe employs harmonic drive gears as a speed reducer. The compact design of the harmonic drive allows for integration directly in the toe joint. In Kengoro [60–62], the toe is actuated by a muscle connected to a 90-W brushless DC motor placed on the lower leg link. It is powerful enough for tiptoe standing, with the help of the hands resting on a wall. In the particular robotic foot of Kuehn *et al.* [59], the motors allow the ankle movement and the movement of the foot via rigid linear segments. In [63], seven motors in hindfoot actuate 20 joints. The structure is divided in seven groups of joints, which are actuated independently. These motors are built in the hindfoot due to the space limitation in the forefoot.

Brushed DC Motors/AC servo: They are used mainly for ankle pitch and roll rotation to change the foot orientation [5, 6, 9, 13, 14, 17–20, 25–28, 31–33, 35–40, 44, 53–55]. In HRP-4 [17] the motor is controlled by two motor drivers in the shin link to make the limb and ankle thin. The ankle of the NAO used an innovative combination of two actuators [25] to make a universal joint module which includes packaging. This reduces the cost while taking into account the mechanical constraints imposed by the outer shell. In WL-12RVII [5,6], AC servo motors are used for antagonistic driven joints to maintain high torque during high-speed revolution, and they coupled harmonic gears (because of their light weight) to each motor. In contrast, in HRP-4C [48], UT- μ 2 [44] and H6 [42, 43], DC motors allow both ankle and foot joints rotation [42–44, 48]. In H6 [42, 43], small and light motors are adopted for the toe joint.

Series elastic actuators: Unlike all other humanoids considered, in the NASA’s first bipedal humanoid robot Valkyrie [23], the ankle actuators are series elastic actuators (SEA). Each ankle is actuated as a pair of parallel linear SEAs to allow for parallel actuation across two DoF. The SEAs directly drive a roller screw nut and feature a two-force member to allow actuation across two degrees of freedom.

Pneumatic actuators: They are used in the internal joints of some robotic feet [45, 45, 46, 52, 58]. In particular, in BIPMAN [45] and PNEUMAT-BH [46, 47], the actuators allow the rotation of the toe pitch, whereas in PNEUMAT-BB [52] they allow the movement of two DoF in midfoot and forefoot. In the Yoon *et al.* structure [58], two upper platforms and three limbs are driven by four pneumatic actuators. This design generate motion between the forefoot and hindfoot and two rotations about the ankle joint allowing natural motions for the foot and ankle. However, pneumatic actuators have two limitations: an inflation speed insufficient to manage strong perturbations and a significant cluttered space.

In the human foot there are many muscles to articulate the foot, allowing a very high number of movements. Inspired by the human foot, some robotic feet have multiple degrees of freedom. Yet, actuating each joint individually can be complex, requiring a large number of actuators. In fact, small rotations and translations between the phalanges of the foot can be obtained thanks to a high number of DoF

14 *I. Frizza, K. Ayusawa, A. Cherubini, H. Kaminaga, P. Fraisse, G. Venture*

Table 3. Sensors to measure ground reaction force, foot tilt angle, displacement, ground detection and pressure.

| | Ground Reaction Force | | Tilt Angle | | Displacement |
|--------------------------------|---------------------------------|-----------------------|------------------------------------|----------------------------|----------------------------------|
| | [10–12] BHR-2 ^{OF} | Potentiometers | [46, 47] Pneumat-BH ^{A,F} | Potentiometers | [5, 6] WL-12RVII ^F |
| | [13, 14] HRP-2 ^{OF} | | [52] Pneumat-BB ^{A,F} | Accelerometers | [10–12] BHR-2 ^F |
| | [15] WALK-MAN ^{OF} | Accelerometers | [10–12] BHR-2 ^F | | [23, 24] VALKYRIE ^F |
| | [16] P2 ^F | | [5, 6] WL-12RVII ^F | Gyroscopes | [10–12] BHR-2 ^F |
| | [17] HRP-4 ^{OF} | Gyroscopes | [10–12] BHR-2 ^F | | [23, 24] VALKYRIE ^F |
| | [21] PYRENE ^{OF} | | [7, 8] PYRENE ^A | Encoders | [34] iCub ^F |
| | [22] JAXON ^{OF} | | [13, 14] HRP-2 ^A | Resistors | [45] BIPMAN ^F |
| | [23, 24] VALKYRIE ^{OF} | | [21] PYRENE ^A | Proximity | [59] ^F |
| 6-axis F/T Sensors | [29, 30] ASIMO ^A | | [23, 24] VALKYRIE ^A | | |
| | [35] ^{OF} | | [25–28] NAO ^A | Ground detection | |
| | [36–40] ^{OF} | Encoders | [31] Ken ^F | Accelerometers | [59] ^F |
| | [41] DRC-HUBO+ ^{OF} | | [34] iCub ^F | Inclination Sensors | [19, 20] KHR-3 ^F |
| | [45] BIPMAN ^{OF} | | [49] ARMAR-4 ^{A,F} | Load Cells | [52] Pneumat-BB ^{OF} |
| | [48] HRP-4C ^{OF} | | [50, 51] LOLA ^{A,F} | | [49] ARMAR-4 ^{UF} |
| | [49] ARMAR-4 ^{OF} | | [59] ^F | Micro Swiches | [5, 6] WL-12RVII ^{UF} |
| | [50, 51] LOLA ^F | | [63] ^F | Optical sensors | [63] ^F |
| | [59] ^{OF} | Inclination | [5, 6] WL-12RVII ^F | | |
| | [53–55] Wabian-2R ^{OF} | | | Pressure | |
| 3-axis F/T Sensors | [19, 20] KHR-3 ^{OF} | | | Pressure Sensors | [23, 24] VALKYRIE ^F |
| Strain Gauge | [44] UT- μ 2 ^F | | | | [45] BIPMAN ^F |
| | [32, 33] ROBIAN ^F | | | | [46, 47] Pneumat-BH ^F |
| | [42, 43] H6 ^{OF} | | | | [52] Pneumat-BB ^F |
| Force sensing resistors | [59] ^{OF} | | | | |
| Torque Sensors | [34] iCub ^{OF} | | | | |
| Load Cells | [60–62] Kengoro ^F | | | | |
| | [52] Pneumat-BB ^{OF} | | | | |
| Pressure Sensors | [44] UT- μ 2 ^F | | | | |

^A Sensor positioned in the ankle

^F Sensor integrated in the foot structure

^{OF} Sensor positioned on the foot

^{UF} Sensor positioned under the foot

without actuation. High DoF allows a high degree of deformability and adaptability to the ground even when the level of control reaches the ankle joint and do not arrive to the foot. In fact, the deformability of the foot makes the kinematics/dynamics hard to model and often to control. Figure 4 shows the variation of the robotic feet degree of actuation (i.e., the number of joints actuated in the foot structure – not considering the ankle) with respect to its DoF. The figure shows the structures constituted by at least two segments: completely flat feet (without any DoF) are not shown. As the figure shows, most robotic feet have an internal joint, the pitch toe. These feet are highlighted in two groups. In the first group (green circle), the joint is passive, whereas feet in the second group (orange circle) have an active toe joint. Moreover, the figure shows that when the DoF increase there is no increase in the number of active joints, but only some of these joints are active. In fact, in [58] and [59], only two of the four degrees of freedom are active. In humanoid

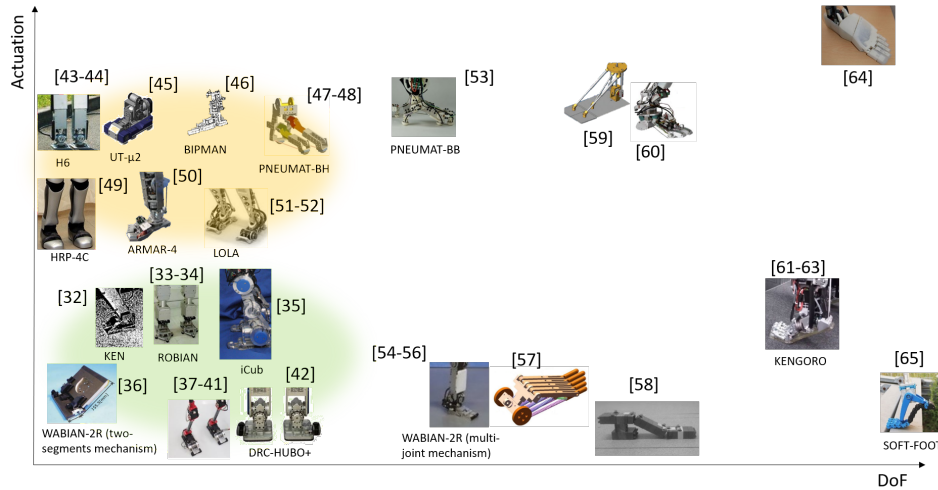


Fig. 4. Trend of the actuation level with respect to the number of degrees of freedom (considering robotic feet with at least one degree of freedom).

foot [60–62], only 1 of the total 16 DoF is active. In structure [63], there are 20 total DoF within the foot, 7 of which are actuated. Finally, [64] has the highest number of DoF, none of which actuated. This structure, tested on the humanoid HRP-4 [78], offers non-actuation together with high deformability.

3.8.5. Sensorization

Ground Reaction Force (GRF): In most humanoids, the GRF and the zero moment point (ZMP) are measured by force/torque (F/T) sensors. As Table 3 shows, most use 6-axis F/T sensors. In WALK-MAN [15], P2 [16], HRP-4 [17, 18], HRP-4C [48], JAXON [22], ASIMO [29, 30], Ogura *et al.* foot [35], Eldirdry *et al.* foot [36–40] and DRC-HUBO+ [41], this unit is composed only of a six-axis force/torque sensor capable of measuring the Zero Moment Point (ZMP) and the GRF. In DRC-HUBO+ [41] each sensor is made of a three-beam cross type structure and can measure three-axis moments of up to $80Nm$ and three axial forces of up to $2000N$ considering the mass of the robot. Six-axis F/T sensors are also employed in BHR-2 [10–12], PYRENE [21], VALKYRIE [23, 24], BIPMAN [45], ARMAR-4 [49], LOLA [50, 51], Kuehn *et al.* foot [59] and WABIAN-2R (multi-joint mechanism) [53–55]. The robotic feet designed by Kuehn *et al.* [59] are equipped not only with a 6-axis F/T sensor but also with a highly articulated sensor structure, to monitor the state of the foot and its interaction with the external environment. A matrix of 49 force sensing resistors (FSR) is installed: 43 sensors measure the GRF at the foot sole and the 6 others measure the impact force of the collision of the foot with the ground. NAO [25] is also equipped with four force sensitive resistors (FSRs) under each foot.

Yet, rather than measuring GRF, they estimate walking qualitative states and fall scenarios. Some robots employ three-axis F/T sensors to measure both ZMP and GRF. It is the case of KHR-3 [19, 20] and UT- μ 2 [44]. In KHR-3 [19, 20], these sensors measure the normal force with the ground F_z and the moments along the walking direction N_x and the transverse direction N_y . UT- μ 2 [44] adopts four 3-axis force sensors in the foot, which enable the robot to measure 6-axis force/torque, avoiding the use of the 6-axis force sensors. In fact, 6-axis force sensors are too large with respect to the size of UT- μ 2. UT- μ 2 adopts also pressure sensors for higher detection. In H6 [42] and in ROBIAN [32, 33], ZMP and vertical reaction forces are measured using strain gauges. In particular, in H6 the system consists of several measurement units distributed in the foot, each with a ground contacting cylinder and a beam with strain gauge. The torques around the x and y axis and the force along the z (vertical) axis are calculated from the output of these units, to obtain the ZMP. In iCub [34], a torque sensor in the foot-ankle system measures the torque generated at the output of the actuators. GRF can also be measured with multiple loadcells, as in Kengoro [60] and in PNEUMAT-BB [52]. In Kengoro [60], the measuring unit is made up of 12 loadcells installed on each foot, 5 on the tip of each toe, 5 on the base of each toe and 2 on the heel. Each unit is loaded through the polyurethane which connects the whole sole of the foot. In PNEUMAT-BB [52] there are three load cells for each foot: one in the hindfoot, one in the the midfoot, and the last one in the forefoot, to measure GRF while walking.

Tilt Angle: As Table 3 shows, most humanoids adopt multiple magnetic encoders to measure the ankle tilt angle, hence the foot orientation. In particular, in iCub [34] the sensor system uses optical encoders to measure the configuration of the foot (linear and rotational position). In some of the feet structures, encoders also provide angle of the internal joints. This is the case of Davis *et al.* [63] and Kuehn *et al.* [59] feet. Davis *et al.* foot [63] offer small local Hall effect sensors to measure the joint angles. In Kuehn *et al.* [59] structure, there are magnetic angular absolute encoders to measure the angles between the different components of the foot. Pneumat series [46, 47, 52] use potentiometers to measure the joint angles. These are located in the joints in the ankle and in the feet. BHR-2's foot [10] estimates the attitude via MEMS accelerometers and angular rate gyroscopes. The sensors can provide the overall orientation of the foot. Finally, WL-12RVII [5, 6] relies on an inclination sensor to measure the ankle tilt angle.

Displacement: The feet are sometimes equipped with linear displacement's sensors as shown in Table 3. BIPMAN [45] adopts linear resistors. Valkyrie [23] adopts three-axis accelerometers and three-axis gyroscopes in the feet. In the feet of Yamaghuchi *et al.* [5] the displacement is measured by four linear potentiometers placed on the surface of the foot at the four corners of its rectangular shape. As previously mentioned, in BHR-2 foot [10], the attitude estimation system uses MEMS accelerometers and angular rate gyroscopes, both for the orientation and linear displacement of the foot. In the iCub foot [34], one optical encoder monitors the position of the motor, while two absolute magnetic encoders measure the position

of the input pulley (harmonic drive output) and the position of the three-spoke structure (the output of the compliant module). Kuehn *et al.* structure [59] uses an infra-red proximity sensor inside the heel.

Ground detection: As Table 3 shows, few humanoids adopt sensors to detect the moment of contact with the ground [80]. KHR-3 [19] adopts inclinometers, Kuehn *et al.* [59] use accelerometers and PNEUMAT-BB [52] adopts load cells, to measure the moment of the detection and the GRF. WL-12RVII [5, 6] uses micro switches and in the foot sole of ARMAR-4 [49] there are seven strain gauge load cells. In the foot of Davis *et al.* [63], optical sensors are used to determine the height of the obstacle on the ground.

Pressure: Four of the surveyed robots are equipped with pressure sensors, as Table 3 shows. In the BIPMAN [45] and in Valkyrie [23], pressure sensors measure the differential pressure between the two chambers of the foot. In the PNEUMAT series [46, 47, 52], the inner pressure of the pneumatic muscles is measured by pressure sensors attached to the plantar pneumatic muscles.

Sensor positioning: Table 3 shows the positioning of the sensors of ankle-foot structures. The sensors can be situated under the sole of the foot, integrated in the foot structure, on the foot structure (between the foot and the ankle) or in the ankle joint. As already mentioned in Sec. 3.5, the majority of structures measure GFR with a force/torque sensor. This sensor is almost always located on the foot structure even if, in this case, the GFR measurement must be corrected by subtracting the dynamic quantity added to the foot posture at each moment, due to the gravity acting on the foot. In some of the surveyed feet, the sensor is inserted directly in the foot structure [16, 32, 33, 44, 50, 51, 60–62]. The tilt sensors are always placed in the joints of the ankle or in the joints inside the foot or in both, to measure a gradient of the landing surface. To measure the feet linear displacement, all robotic feet have the sensors positioned in the foot. To detect the heel strike during walking, WL-12RVII [5, 6] and ARMAR-4 [49] adopt sensors under the foot. WL-12RVII has microswitches with levers in the four corners of the lower surface of the lower-foot plate. Under each foot of ARMAR-4, there are seven strain gauge load cells. The feet of KHR-3 [19, 20] and the feet of [59] [63] have sensors placed inside the foot structure. Only in PNEUMAT-BB [52] load cells are on the hindfoot, the midfoot, and the forefoot, to detect the heel strike while walking. Pressure sensors are always placed in the foot structure [23, 24, 46, 47, 52, 81, 81].

As most feet are flat, the sole sensors used are for those for the whole body balance control to guarantee stability during balancing and walking. F/T sensors with strain gauges are commonly used to perform both feedback control and gait performance analysis. Usually, they are positioned on the foot as Table 3 shows. However, the mass of the F/T sensor at the leg end increases the leg inertia and it can create noise under heavy impacts and fast movements. Therefore, such sensors were found unsuitable for high-speed locomotion [82]. A lighter and cheaper alternative to F/T sensors are GRF and ZMP sensors on the insole plane. FSR can

be used to estimate walking states but their accuracy is usually too low to allow for GRF estimation, they may be unsuitable for heavy robots and for fall detection. Other sensors are marginally used. Sensor placement is also very homogeneous in all systems, mainly due to operational constraints.

3.8.6. *Models*

Point, semicircular, triangular or unique-segment feet model: Most publications in the literature rely on a model of the bipedal robot in which the foot is modeled as a point. However, it is possible to find other models of the foot: semicircular feet [83], rigid segment [84] or triangle in which the vertices represent the ankle, heel and toe [85–89]. In most of the feet classified in Sec. 3, dynamic elements are not considered. Considering robotic flat feet, research groups of CASSIE [7, 8], WABIAN-2R (unique-segment mechanism) [9], KHR-3 [19, 20], PYRENE [21], JAXON [22], VALKYRIE [23, 24], NAO [25–28] and ASIMO [29, 30] did not develop a dynamic model of the foot to be included in the total bipedal model. In other robots, however, some research groups have developed a dynamic model of the soft material present in the sole of the robot, including the elastic elements. This is the case for LOLA [50], ROBIAN [32, 33], Kengoro [60–62], WALK-MAN [15], P2 [16], BHR-2 [10–12], DRC-HUBO+ [41], WL-12RVII [5, 6], HRP-2 [13, 90] and HRP-4 [17, 18] where the elastic materials are modeled as linear visco-elastic elements with negligible mass. Kuhen *et al.* [59] researchers implemented the concept of virtual springs in both DoFs due to adaptation of the foot sole to improve ground contact and active damping of shocks. Some of the feet with internal joints, such that of iCub [34], WABIAN-2R (two-segments and multi-joint mechanisms) [35, 53–55], Ken [31] and the structures [56, 57] are modeled with a single rigid segment, even if the structure includes multiple passive joints.

Multiple-segments feet model: models allow to calculate the kinematic parameters of the foot during walking [57, 91, 92]. Park *et al.* [92] developed a five segments foot model with four 3 DoFs joints between the segments. This type of model is more accurate in reproducing the shape of the foot and its functionality improves stability since there are many points of contact between the foot and the ground. Also the feet of in Elidiry *et al.* foot [36–40], in Ken [31] are modeled considering the internal pitch joint of the toe. For example, in HRP-2TJ [74], the feet include an internal passive joint. The passive joint is often described by a simple mass-spring-damper system *et al.* [36–40, 74]. In Ken [31], authors modeled the toe joint as a free joint because the friction force needed by the toe is sufficient to avoid foot slipping. Researchers develop a model of the interaction between the ground and the deformable (multiple-segment) feet model in the quasi-static phase of the walk for SoftFoot [93]. They simplify the structure in two dimensions, but they consider all the links and pulleys that make up the plantar fascia and the internal tendon passed between the structure. The model is used to estimate the distribution of contact forces between the foot and the ground, by using instead of the equation of

motion, the quasi-static equilibrium of feet.

During normal locomotion, the foot is the last segment of the leg kinematic chain and it is fundamental in the study of walking stability. Indeed, the dynamics of the foot have a strong influence on the walking performance. However, only a small amount of detailed literature exists that incorporates the foot model in the complete model of the biped and few walk controllers include the foot dynamics. In most cases, foot dynamics is ignored, although it plays a fundamental role in the dynamics of a humanoid robot. When the structure of the feet is more complex, it is not easy to develop an approximate dynamic model of the system. For this reason, most humanoid robot control systems do not consider the foot dynamics. In fact, for the development of the control design, it is very important to take into consideration stability, robustness with regards to uncertain parameters like the ground irregularity, and precision to follow the trajectory. In summary, with increasing DoF of the foot, the number of controlled joints not always increases due to the control complexity.

4. Suggested future developments

In this section we propose a selection of possible areas of investigation that could lead to major breakthroughs in the development of robotic feet.

4.1. *Inspirations from animals feet*

While most of the inspiration for bipedal robot feet comes from human feet, interestingly other animals (both terrestrial and aquatic) have also inspired some new designs for robotic feet. For example, recent works are inspired by ducks [94], birds [7, 8, 95], geckos [96], frogs [97], or salamanders [98, 99]. In fact, animal movement has several advantages such as high efficiency and high mobility on extremely varied terrains.

Pillearachchige *et al.* proposed a claw inspired from birds [95]. It reproduces their ability to walk, swim and cling to the ground. It consists of four fingers, formed respectively by one, two, three and four phalanges, which can open and close.

The foot of the bipedal robot Cassie is also inspired by a bird's foot [7, 8]. Indeed, the morphology and the name of the robot are inspired by the Cassowary, a flightless bird native to New Guinea, comparable to an ostrich. Its knees, attached to a short torso, are reversed with respect to human ones.

Inspirations from aquatic and amphibious animals is of particular interest. Underwater walking requires higher energy efficiency than walking on land. Animals such as salamanders [98, 99], frogs [97] or ducks [94], have particularly efficient feet for walking on ground and underwater. The structure of their feet generates high forces. Imitating such structures for the realization of robotic feet could be of major interest. For example, the salamander feet contribute significantly to the thrust of the body, by increasing the contact with the fingers, reducing the kinematics of

the limbs, and consuming less energy [100]. Paez *et al.* proposed a mechanism that mimics salamander feet [98]. This particular foot is very interesting because it has directional flexibility. Depending on the activation of the motor, it can be rigid or highly yielding. This way, the foot can generate variable stiffness, and adapt to sudden change in the terrain.

Moreover, Ijsperit *et al.* presented a spinal cord model and its implementation in an amphibious salamander robot and they show the robot's ability to switch from aquatic to terrestrial locomotion [99]. Shimizu *et al.* proposed a webbed robotic foot inspired by a frog's foot [97]. Frog's feet toes can only bend in the direction of plantar flexion. This foot consists of a surface with cuts in the center of the toes and around the root of the toes. These cuts are crucial in the rotation joints. A soft rubber is applied to the sole of the foot. With this design, even this robotic foot can only bend in the direction of plantar flexion, like the frog's foot. This type of robotic foot produces propulsive force, passively reducing the drag force that resists the robot walk.

Finally, the authors of [94] developed a robot that uses webbed duck feet to walk on different terrains, swim in the water and face obstacles in its path. In their design, two flaps are attached to the feet bottom with hinges, so they open and close with the water flow. The foot can be rotated at the ankle with the help of a servomotor to change modes: swimming or walking. In walking mode, at least two feet are always in contact with the ground at the same time. In swim mode, the flaps close when pushed back and open when the feet move forward.

Another area in which inspirations from animals is important for robotic feet is that of the development of new materials.

4.2. Soft material in robotic feet

In recent years, the integration of soft materials within conventional robotics has sparked a wave of enthusiasm. Robotic feet could use this type of materials. Indeed, thanks to their adaptability to uneven terrain and intrinsic safety the introduction of soft materials offers the possibility to overcome many issues inherent in conventional robots. Works in this area are also often inspired by animals such as octopus [101, 102], benthic animals [103], geckos or inchworms [104]. Geckos are the largest animals capable of performing unassisted vertical hikes. Development of dry adhesive materials to be used as feet for climbing robots has been the focus of [105, 106]. Yet, on each foot the areas of dry adhesive material must be large enough to support the robot weight during locomotion. To improve the use of the adhesive material for heavier applications, a hybrid soft-rigid foot with a sandwich structure is proposed in [96]. It consists of three main layers (parts in hard, soft and dry adhesive material). With the rigid part, the foot generates sufficient pressure to obtain an adhesive force. The soft part maximizes the adhesive area. Finally, the dry adhesive material provides strong adhesion. The octopus is one of the most studied animals in soft robotics [101, 102]. Indeed, the muscle in its arm provides everything

necessary for moving. Laschi developed a robot called Octobot [102], taking inspiration from the octopus. This robot has eight sinuous arms, which work together not only for the robot's locomotion, but also for grasping objects. This robot mimics the octopus's jet propulsion method for swimming. The researchers completed impressive tests with Octobot swimming in the waters of the Mediterranean Sea. Soft robots inspired by animals are advantageous for carrying out various activities such as climbing on curvilinear, flat or vertical surfaces [104] or walking on the seabed inside a fluid [103]. Others are developed to grasp objects [107,108], including very thin and flexible ones [109]. Most of these robots use soft materials for actuation. For example, shape memory alloy (SMA) wires [104], fabric reinforced textile actuators (FRTA) [108], dielectric elastomer actuators (DEA) generate compression loads by performing morphing of the shape [110] or McKibben artificial muscles [101]. Pressurized chambers make up the limbs of the robot which, if implemented with a given sequence, can activate the walking gait [103]. Inspired by natural muscles, a challenge in modern robotics is the development of autonomous soft actuators. Some of these are already used in the development of robot hands [101,108] and in the near future, they could be used on robotic feet. Soft materials could be included in the robotic foot structure, since they offer several advantages also in the field of locomotion. Indeed, the shock with the ground during walking can be absorbed by soft materials. Materials of this type allow a greater adaptation to uneven surfaces even in underwater environments [104].

With the use of soft materials, it could be possible to distribute the contact pressure [107]. Robotic feet could be covered with soft skin, which deforms according to the movement of the structure. The soft skin is capable of increasing the local contact area, in order to disperse the contact pressure over the entire surface. Thinking about multi-joint foot structures, we could get more advantage because the deformation of the soft skin is dispersed due to the small angular variation of each joint and there will be no concentration of local elongation and subsidence. If the DoF of a skeleton structure are limited, they cannot follow the shape of the object because the contact area is limited, even if there is a flexible exterior on the contact surface. Robotic feet could take advantage of the inherent compliance and high flexibility of materials to create highly adaptable robots [103]. Robots that use these components can adapt to their environments, allowing compliance with uneven surfaces. This behavior is particularly useful for walking systems, since a soft actuator can bend to various shapes that would require many joints to replicate rigidly. Moreover, following the idea of human-like performance, some soft actuators can contract like human muscles by applying pressure [81,101,103,108].

Soft materials could also be useful in sensorization. Soft sensing techniques were explored by Park *et al.* in the form of a custom strain sensor developed in an active soft orthotic device [111]. Subsequently, this device, in combination with a hyperelastic pressure sensor [112] made it possible to construct a soft artificial skin with conductive channels of liquid metal, capable of multimodal detection

[113]. Exoskeletal end effectors implanted with fiber-optic Bragg grating sensors allowed Park et al. to incorporate the GRF detection, while limiting the mass of the sensors [114]. The Cheetah four-legged MIT robot features a new footpad design for GRF measurement including tactile sensing [115]. Using a soft material sensor, this system is also capable of shock absorption thanks to its soft materials.

4.3. *Sensory system for robotic feet*

As we have shown in Sections 3.8.5 and 3.8.6, the modeling and the sensorization of robotic feet is paramount to the success of efficient controllers. Recently, a plantar skin composed of hexagonal cells was introduced by Rogelio *et al.* [116]. Each cell provides four sensing modalities (force, pre-touch, acceleration and temperature). Authors mounted forty-two cells in each sole of the REEM-C robot and computed the pressure distribution to acquire the support polygon shape using the normal force sensors. With this additional information, balance and walking controllers could adapt online the kinematic constraints, to ensure stability. Comparing experimental results between force/torque sensors and plantar robot skin performances, the authors of [116] observe that with force/torque sensors the balance controller does not have enough information to re-plan steps when an obstacle is detected under the foot while walking. Indeed, with only the measure of the moment produced at the ankle by the collision, the robot falls down. Instead, the balance controller with skin information can decide when to re-plan steps, since it provides the support polygon area.

Also in the human body, the perception of information from sensory elements in the foot is very important. Indeed, in the human body the sensory touch particles allocated in the foot are fundamental both for balance and for locomotion. They are placed in the skin along the plantar area and they are connected with three main nerves that coordinate reflexes and muscle groups during walking. Sensitivity depends on the walking phase and it is different between support and swing leg.

In conclusion, recent research studies about sensorization are trying to provide not only the GRF, but also the shape of the pressure distribution and the support polygon, to improve the stability in walking and balancing performance. Many developments in this area are yet to come.

5. Conclusions

This paper surveyed different types of robotic feet existing in the literature. We classified robotic feet according to strategy, structure, number of degrees of freedom (DoF), actuation method for ankle and foot, type of actuator, sensorization, and integration of the foot in the robot model/controller.

We could observe that most robotic feet are designed with a zero DoF plate but, to improve the walking on uneven terrain, some humanoid robots adopt layers of elastic materials under the foot sole. Although some designers have added one or more joints to the feet to improve balance and walk on rough terrain, there are

still few multi-segment structures. Moreover, comparing the surveyed feet, we could observe that when the number of DoF increase, there is no increasing in the number of active joints. Indeed, only some of these joints are active. Finally, we can conclude that the challenge to include foot dynamics in the walk controllers of biped robots is still open due to the complexity of developing the foot model and designing the walking controller.

Acknowledgements

The authors would like to thank Jin'ichi Yamaguchi, Kenji Hashimoto, Nikolaos Tsagarakis, Olivier Stasse, Yu Ogura, Koichi Nishiwaki, Marina Guihard, Tamin Asfour, Thomas Buschmann, Byung-Ju Yi, Daniel Kuhlen, Yuki Asano and Darwin Caldwell for the collaboration in providing the pictures.

The research presented in this article was carried out as part of the SOPHIA project, which has received funding from the European Union's Horizon 2020 research and innovation programme under Grant Agreement No. 871237.

References

1. J. Hodgins, "Legged robots on rough terrain: experiments in adjusting step length," in *Proceedings. 1988 IEEE International Conference on Robotics and Automation*. IEEE, 1988, pp. 824–826.
2. J. K. Hodgins and M. H. Raibert, "Adjusting step length for rough terrain locomotion," *Dynamically Stable Legged Locomotion*, p. 27, 1991.
3. "Coastline orthopaedic associates (anatomy of the foot and ankle) website," <https://www.coastlineortho.com/>, accessed: 2020-06-30.
4. J. J. Fraser, M. A. Feger, and J. Hertel, "Midfoot and forefoot involvement in lateral ankle sprains and chronic ankle instability. part 1: anatomy and biomechanics," *IJSPT*, vol. 11, no. 6, p. 992, 2016.
5. J. Yamaguchi, A. Takanishi, and I. Kato, "Experimental development of a foot mechanism with shock absorbing material for acquisition of landing surface position information and stabilization of dynamic biped walking," in *ICRA*, vol. 3, 1995, pp. 2892–2899.
6. J. Yamaguchi and A. Takanishi, "Multisensor foot mechanism with shock absorbing material for dynamic biped walking adapting to unknown uneven surfaces," in *MFI*, 1996, pp. 233–240.
7. J. Reher, W.-L. Ma, and A. D. Ames, "Dynamic walking with compliance on a cassie bipedal robot," in *European Control Conf.*, 2019, pp. 2589–2595.
8. Z. Li, C. Cummings, and K. Sreenath, "Animated cassie: A dynamic relatable robotic character," *arXiv preprint arXiv:2009.02846*, 2020.
9. H.-j. Kang, K. Hashimoto, H. Kondo, K. Hattori, K. Nishikawa, Y. Hama, H.-o. Lim, A. Takanishi, K. Suga, and K. Kato, "Realization of biped walking on uneven terrain by new foot mechanism capable of detecting ground surface," in *2010 ICRA*, 2010, pp. 5167–5172.
10. J. Li, Q. Huang, W. Zhang, Z. Yu, and K. Li, "Flexible foot design for a humanoid robot," in *ICAL*, 2008, pp. 1414–1419.
11. Z. Peng, Y. Fu, Z. Tang, Q. Huang *et al.*, "Online walking pattern generation and system software of humanoid bhr-2," in *IROS*, 2006, pp. 5471–5476.

24 *I. Frizza, K. Ayusawa, A. Cherubini, H. Kaminaga, P. Fraisse, G. Venture*

12. Z. Yu, Q. Huang, J. Li, Q. Shi, X. Chen, and K. Li, “Distributed control system for a humanoid robot,” in *ICRA*, 2007, pp. 1166–1171.
13. K. Kaneko, F. Kanehiro, S. Kajita, K. Yokoyama, K. Akachi, T. Kawasaki, S. Ota, and T. Isozumi, “Design of prototype humanoid robotics platform for hrp,” in *IROS*, vol. 3, 2002, pp. 2431–2436.
14. N. Kanehira, T. Kawasaki, S. Ohta, T. Ismumi, T. Kawada, F. Kanehiro, S. Kajita, and K. Kaneko, “Design and experiments of advanced leg module (hrp-2l) for humanoid robot (hrp-2) development,” in *IROS*, vol. 3, 2002, pp. 2455–2460.
15. F. Negrello, M. Garabini, M. G. Catalano, P. Kryczka, W. Choi, D. G. Caldwell, A. Bicchi, and N. G. Tsagarakis, “Walk-man humanoid lower body design optimization for enhanced physical performance,” in *ICRA*, 2016, pp. 1817–1824.
16. K. Hirai, M. Hirose, Y. Haikawa, and T. Takenaka, “The development of honda humanoid robot,” in *ICRA*, vol. 2, 1998, pp. 1321–1326.
17. K. Kaneko, F. Kanehiro, M. Morisawa, K. Akachi, G. Miyamori, A. Hayashi, and N. Kanehira, “Humanoid robot hrp-4-humanoid robotics platform with lightweight and slim body,” in *IROS*, 2011, pp. 4400–4407.
18. S. Caron, A. Kheddar, and O. Tempier, “Stair climbing stabilization of the hrp-4 humanoid robot using whole-body admittance control,” in *ICRA*, 2019, pp. 277–283.
19. I.-W. Park, J.-Y. Kim, J. Lee, and J.-H. Oh, “Mechanical design of humanoid robot platform khr-3 (kaist humanoid robot 3: Hubo),” in *Humanoids*, 2005, pp. 321–326.
20. I.-W. Park, J.-Y. Kim, and J.-H. Oh, “Online biped walking pattern generation for humanoid robot khr-3 (kaist humanoid robot-3: Hubo),” in *Humanoids*, 2006, pp. 398–403.
21. O. Stasse, T. Flayols, R. Budhiraja, K. Giraud-Esclasse, J. Carpentier, J. Mirabel, A. Del Prete, P. Souères, N. Mansard, F. Lamiroux *et al.*, “Talos: A new humanoid research platform targeted for industrial applications,” in *Humanoids*, 2017, pp. 689–695.
22. K. Kojima, T. Karasawa, T. Kozuki, E. Kuroiwa, S. Yukizaki, S. Iwaishi, T. Ishikawa, R. Koyama, S. Noda, F. Sugai *et al.*, “Development of life-sized high-power humanoid robot jaxon for real-world use,” in *Humanoids*, 2015, pp. 838–843.
23. N. A. Radford, P. Strawser, K. Hambuchen, J. S. Mehling, W. K. Verdeyen, A. S. Donnan, J. Holley, J. Sanchez, V. Nguyen, L. Bridgwater *et al.*, “Valkyrie: Nasa’s first bipedal humanoid robot,” *JFR*, vol. 32, no. 3, pp. 397–419, 2015.
24. N. Paine, J. S. Mehling, J. Holley, N. A. Radford, G. Johnson, C.-L. Fok, and L. Sentis, “Actuator control for the nasa-jsc valkyrie humanoid robot: A decoupled dynamics approach for torque control of series elastic robots,” *JFR*, vol. 32, no. 3, pp. 378–396, 2015.
25. D. Gouaillier, V. Hugel, P. Blazevic, C. Kilner, J. Monceaux, P. Lafourcade, B. Marnier, J. Serre, and B. Maisonnier, “The nao humanoid: a combination of performance and affordability,” *CoRR abs/0807.3223*, 2008.
26. —, “Mechatronic design of nao humanoid,” in *ICRA*, 2009, pp. 769–774.
27. D. Gouaillier, C. Collette, and C. Kilner, “Omni-directional closed-loop walk for nao,” in *Humanoids*, 2010, pp. 448–454.
28. J. Strom, G. Slavov, and E. Chown, “Omnidirectional walking using zmp and preview control for the nao humanoid robot,” in *Robot Soccer World Cup*. Springer, 2009, pp. 378–389.
29. M. Hirose and K. Ogawa, “Honda humanoid robots development,” *Philosophical Transactions of the Royal Society A: Mathematical, Physical and Engineering Sciences*, vol. 365, no. 1850, pp. 11–19, 2007.
30. Y. Sakagami, R. Watanabe, C. Aoyama, S. Matsunaga, N. Higaki, and K. Fujimura,

- “The intelligent asimo: System overview and integration,” in *IEEE IROS*, vol. 3, 2002, pp. 2478–2483.
31. T. Takahashi and A. Kawamura, “Posture control using foot toe and sole for biped walking robot” ken”,” in *AMC*, 2002, pp. 437–442.
 32. F. Ouezdou, A. Konno, R. Sellaouti, F. Gravez, B. Mohamed, and O. Bruneau, “Robian biped project: A tool for the analysis of the human being locomotion system,” *Proc. Int. Congr. Climbing Walking Robots*, pp. 375–382, 2002.
 33. A. Konno, R. Sellaouti, F. B. Amar, and F. B. Ouezdou, “Design and development of the biped prototype robian,” in *IEEE ICRA*, vol. 2, 2002, pp. 1384–1389.
 34. N. G. Tsagarakis, Z. Li, J. Saglia, and D. G. Caldwell, “The design of the lower body of the compliant humanoid robot “ccub”,” in *ICRA*, 2011, pp. 2035–2040.
 35. Y. Ogura, K. Shimomura, H. Kondo, A. Morishima, T. Okubo, S. Momoki, H.-o. Lim, and A. Takanishi, “Human-like walking with knee stretched, heel-contact and toe-off motion by a humanoid robot,” in *IROS*, 2006, pp. 3976–3981.
 36. O. Eldirdiry, R. Zaier, F. Alnajjar, A. Al-Yahmedi, and I. Bahadur, “Foot modelling for investigating foot-drop problem using biomechanical legs,” in *ASET*, 2019, pp. 1–6.
 37. O. Eldirdiry, R. Zaier, A. Al-Yahmedi, I. Bahadur, and F. Alnajjar, “Modeling of a biped robot for investigating foot drop using matlab/simulink,” *Simulation Modelling Practice and Theory*, vol. 98, p. 101972, 2020.
 38. O. Eldirdiry and R. Zaier, “Modeling biomechanical legs with toe-joint using simscape,” in *ISMA*, 2018, pp. 1–7.
 39. O. Eldirdiry, R. Zaier, I. Bahadur, A. Al-Yahmedi, and A. Boudaka, “Towards foot-drop correction using a simulation of bio-inspired robotic legs,” in *ICARM*, 2019, pp. 780–785.
 40. R. Zaier and A. Al-Yahmedi, “Design of biomechanical legs with a passive toe joint for enhanced human-like walking,” *TJER*, vol. 14, no. 2, pp. 166–181, 2017.
 41. T. Jung, J. Lim, H. Bae, K. K. Lee, H.-M. Joe, and J.-H. Oh, “Development of the humanoid disaster response platform drc-hubo+,” *IEEE TRO*, vol. 34, no. 1, pp. 1–17, 2018.
 42. K. Nishiwaki, S. Kagami, Y. Kuniyoshi, M. Inaba, and H. Inoue, “Toe joints that enhance bipedal and fullbody motion of humanoid robots,” in *ICRA*, vol. 3, 2002, pp. 3105–3110.
 43. K. Nishiwaki, T. Sugihara, S. Kagami, F. Kanehiro, M. Inaba, and H. Inoue, “Design and development of research platform for perception-action integration in humanoid robot: H6,” in *IROS*, vol. 3, 2000, pp. 1559–1564.
 44. K. Yamamoto, T. Sugihara, and Y. Nakamura, “Toe joint mechanism using parallel four-bar linkage enabling humanlike multiple support at toe pad and toe tip,” in *Humanoids*, 2007, pp. 410–415.
 45. M. Guihard and P. Gorce, “Biorobotic foot model applied to bipman robot,” in *IEEE SMC*, vol. 7, 2004, pp. 6491–6496.
 46. T. Kawakami and K. Hosoda, “Bipedal walking with oblique mid-foot joint in foot,” in *ROBIO*, 2015, pp. 535–540.
 47. M. Shimizu, K. Suzuki, K. Narioka, and K. Hosoda, “Roll motion control by stretch reflex in a continuously jumping musculoskeletal biped robot,” in *IROS*, 2012, pp. 1264–1269.
 48. K. Kaneko, F. Kanehiro, M. Morisawa, K. Miura, S. Nakaoka, and S. Kajita, “Cybernetic human hrp-4c,” in *Humanoids*, 2009, pp. 7–14.
 49. T. Asfour, J. Schill, H. Peters, C. Klas, J. Bückner, C. Sander, S. Schulz, A. Kargov, T. Werner, and V. Bartenbach, “Armar-4: A 63 dof torque controlled humanoid

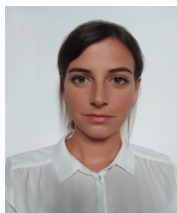
- robot,” in *Humanoids*, 2013, pp. 390–396.
50. S. Lohmeier, T. Buschmann, and H. Ulbrich, “Humanoid robot lola,” in *ICRA*, 2009, pp. 775–780.
 51. T. Buschmann, S. Lohmeier, and H. Ulbrich, “Humanoid robot lola: Design and walking control,” *J. of physiology-Paris*, vol. 103, no. 3-5, pp. 141–148, 2009.
 52. K. Narioka, T. Homma, and K. Hosoda, “Humanlike ankle-foot complex for a biped robot,” in *Humanoids*, 2012, pp. 15–20.
 53. K. Hashimoto, Y. Takezaki, K. Hattori, H. Kondo, T. Takashima, H.-o. Lim, and A. Takanishi, “A study of function of foot’s medial longitudinal arch using biped humanoid robot,” in *IROS*, 2010, pp. 2206–2211.
 54. K. Hashimoto, Y. Yoshimura, H. Kondo, H.-o. Lim, and A. Takanishi, “Realization of quick turn of biped humanoid robot by using slipping motion with both feet,” in *ICRA*, 2011, pp. 2041–2046.
 55. K. Hashimoto, K. Hattori, T. Otani, H.-O. Lim, and A. Takanishi, “Foot placement modification for a biped humanoid robot with narrow feet,” *The Scientific World J.*, vol. 2014, 2014.
 56. J.-T. Seo and B.-J. Yi, “Modeling and analysis of a biomimetic foot mechanism,” in *IROS*, 2009, pp. 1472–1477.
 57. S. Yalamanchili, R. Abboud, and W. Wang, “A model to calculate the joint movements and forces in the foot,” in *ICEMI*, 2009, pp. 4–532.
 58. J. Yoon, H. Nandha, D. Lee, and G.-s. Kim, “A novel 4-dof robotic foot mechanism with multi-platforms for humanoid robot (sice-iccas 2006),” in *SICE-ICASE*, 2006, pp. 3500–3504.
 59. D. Kuehn, F. Beinersdorf, F. Bernhard, K. Fondahl, M. Schilling, M. Simnofske, T. Stark, and F. Kirchner, “Active spine and feet with increased sensing capabilities for walking robots,” in *iSAIRAS*, 2012, pp. 4–6.
 60. Y. Asano, S. Nakashima, T. Kozuki, S. Ookubo, I. Yanokura, Y. Kakiuchi, K. Okada, and M. Inaba, “Human mimetic foot structure with multi-dofs and multi-sensors for musculoskeletal humanoid kengoro,” in *IROS*, 2016, pp. 2419–2424.
 61. Y. Asano, K. Okada, and M. Inaba, “Design principles of a human mimetic humanoid: Humanoid platform to study human intelligence and internal body system,” *Science Robotics*, vol. 2, no. 13, p. eaaq0899, 2017.
 62. Y. Asano, T. Kozuki, S. Ookubo, M. Kawamura, S. Nakashima, T. Katayama, I. Yanokura, T. Hirose, K. Kawaharazuka, S. Makino *et al.*, “Human mimetic musculoskeletal humanoid kengoro toward real world physically interactive actions,” in *Humanoids*, 2016, pp. 876–883.
 63. S. Davis and D. G. Caldwell, “The design of an anthropomorphic dexterous humanoid foot,” in *IROS*, 2010, pp. 2200–2205.
 64. C. Piazza, C. Della Santina, G. M. Gasparri, M. G. Catalano, G. Grioli, M. Garabini, and A. Bicchi, “Toward an adaptive foot for natural walking,” in *Humanoids*, 2016, pp. 1204–1210.
 65. T. McGeer *et al.*, “Passive dynamic walking,” *I. J. Robotic Res.*, vol. 9, no. 2, pp. 62–82, 1990.
 66. K. Goldberg and M. Raibert, “Conditions for symmetric running in single-and double-support,” in *Proceedings. 1987 IEEE International Conference on Robotics and Automation*, vol. 4. IEEE, 1987, pp. 1890–1895.
 67. “Ieee spectrum,” <https://spectrum.ieee.org/033010-hubo-ii-humanoid-robot-is-lighter-and-faster>, accessed: 2022-01-05.
 68. K. Kojima, Y. Kojio, T. Ishikawa, F. Sugai, Y. Kakiuchi, K. Okada, and M. Inaba,

- “Drive-train design in jaxon3-p and realization of jump motions: Impact mitigation and force control performance for dynamic motions,” in *2020 IEEE/RSJ International Conference on Intelligent Robots and Systems (IROS)*. IEEE, 2020, pp. 3747–3753.
69. “bostondynamics website,” <https://www.bostondynamics.com/atlas>, accessed: 2022-01-05.
 70. “bostondynamics video,” <https://slideslive.com/38946802/boston-dynamics>, accessed: 2022-01-05.
 71. C. Neves and R. Ventura, “Survey of semi-passive locomotion methodologies for humanoid robots,” in *Adaptive Mobile Robotics*. World Scientific, 2012, pp. 393–400.
 72. W. Choi, C. Zhou, G. A. Medrano-Cerda, D. G. Caldwell, and N. G. Tsagarakis, “A new foot sole design for humanoids robots based on viscous air damping mechanism,” in *2015 IEEE/RSJ International Conference on Intelligent Robots and Systems (IROS)*. IEEE, 2015, pp. 4498–4503.
 73. K. Miura, M. Morisawa, F. Kanehiro, S. Kajita, K. Kaneko, and K. Yokoi, “Human-like walking with toe supporting for humanoids,” in *IROS*, 2011, pp. 4428–4435.
 74. R. Sellaouti, O. Stasse, S. Kajita, K. Yokoi, and A. Kheddar, “Faster and smoother walking of humanoid hrp-2 with passive toe joints,” in *IROS*, 2006, pp. 4909–4914.
 75. S. Kajita, K. Kaneko, M. Morisawa, S. Nakaoka, and H. Hirukawa, “Zmp-based biped running enhanced by toe springs,” in *ICRA*, 2007, pp. 3963–3969.
 76. A. David, J.-R. Chardonnet, A. Kheddar, K. Kaneko, and K. Yokoi, “Study of an external passive shock-absorbing mechanism for walking robots,” in *Humanoids*, 2008, pp. 435–440.
 77. H. Minakata, “A study of flexible shoe system for biped robot,” in *AMC.*, 2004, pp. 387–392.
 78. M. G. Catalano, I. Frizza, C. Morandi, G. Grioli, K. Ayusawa, T. Ito, and G. Venture, “Hrp-4 walks on soft feet,” *IEEE RA-L*, 2020.
 79. W. Choi, G. A. Medrano-Cerda, D. G. Caldwell, and N. G. Tsagarakis, “Design of a variable compliant humanoid foot with a new toe mechanism,” in *IEEE Int. Conf. on Robotics and Automation*, 2016, pp. 642–647.
 80. L. Wagner, P. Fankhauser, M. Bloesch, and M. Hutter, “Foot contact estimation for legged robots in rough terrain,” in *Advances in Cooperative Robotics*. World Scientific, 2017, pp. 395–403.
 81. B. Aktaş and R. D. Howe, “Flexure mechanisms with variable stiffness and damping using layer jamming,” in *IROS*, 2019, pp. 7616–7621.
 82. M. Y. Chuah, M. Estrada, and S. Kim, “Composite force sensing foot utilizing volumetric displacement of a hyperelastic polymer,” in *IROS*, 2012, pp. 1963–1969.
 83. F. Asano and Z.-W. Luo, “Dynamic analyses of underactuated virtual passive dynamic walking,” in *ICRA*, 2007, pp. 3210–3217.
 84. J. Lee and Y. Oh, “A planar stable walking model based on ankle actuation and the virtual pendulum concept,” in *IROS*, 2016, pp. 5169–5174.
 85. A. B. Pournazhdi, M. Mirzaei, and A. R. Ghiasi, “Dynamic modeling and sliding mode control for fast walking of seven-link biped robot,” in *ICCIA*, 2011, pp. 1012–1017.
 86. P. Channon, S. Hopkins, and D. Pham, “Derivation of optimal walking motions for a bipedal walking robot,” *Robotica*, vol. 10, no. 2, pp. 165–172, 1992.
 87. H. Arnaud and A. Yannick, “Walking gait of a planar bipedal robot with four-bar knees,” *Movement & Sport Sciences-Science & Motricité*, no. 90, pp. 87–97, 2015.
 88. A. Ayari and J. Knani, “Kinematics velocity and dynamic modeling of biped robot,”

28 *I. Frizza, K. Ayusawa, A. Cherubini, H. Kaminaga, P. Fraise, G. Venture*

- in *CoDIT*, 2017, pp. 0849–0854.
89. W. Yu, R. Zhuang, and Z. Shao, “Balance recovery analysis with constraints of feet-ground for biped robot,” in *2017 ICMA*, 2017, pp. 1597–1601.
 90. Y. Mikami, T. Moulard, E. Yoshida, and G. Venture, “Identification of hrp-2 foot’s dynamics,” in *IROS*, 2014, pp. 927–932.
 91. S. Hwang, H. Choi, and Y. Kim, “Motion analysis based on a multi-segment foot model in normal walking,” in *The 26th EMBC*, vol. 2, 2004, pp. 5104–5106.
 92. H. Park, R. Yu, and J. Lee, “Multi-segment foot modeling for human animation,” in *MIG*, 2018, pp. 1–10.
 93. D. Mura, C. Della Santina, C. Piazza, I. Frizza, C. Morandi, M. Garabini, G. Grioli, and M. G. Catalano, “Exploiting adaptability in soft feet for sensing contact forces,” *IEEE RA-L*, vol. 5, no. 2, pp. 391–398, 2019.
 94. S. B. A. Kashem, S. Jawed, J. Ahmed, and A. Iqbal, “An experimental study of the amphibious robot inspired by biological duck foot,” in *2018 IEEE 12th Int. Conf. on Compatibility, Power Electronics and Power Engineering (CPE-POWERENG)*, 2018, pp. 1–6.
 95. K. Pillearchchige, T. Pereira, and K. M. Arif, “Bio-inspired multitasking robotic gripper design and development,” in *IEEE/ASME Int. Conf. on Mechatronic and Embedded Systems and Applications*, 2016, pp. 1–5.
 96. D. Shao, J. Chen, A. Ji, Z. Dai, and P. Manoonpong, “Hybrid soft-rigid foot with dry adhesive material designed for a gecko-inspired climbing robot,” in *IEEE Int. Conf. on Soft Robotics*, 2020, pp. 578–585.
 97. M. Shimizu, D. Ishii, H. Aonuma, and K. Hosoda, “Swimming frog cyborg which generates efficient hydrodynamic propulsion with webbed foot,” in *IEEE Int. Conf. on Cyborg and Bionic Systems*, 2017, pp. 73–76.
 98. L. Paez, K. Melo, R. Thandiackal, and A. J. Ijspeert, “Adaptive compliant foot design for salamander robots,” in *IEEE Int. Conf. on Soft Robotics*, 2019, pp. 178–185.
 99. A. J. Ijspeert, A. Crespi, D. Ryczko, and J.-M. Cabelguen, “From swimming to walking with a salamander robot driven by a spinal cord model,” *science*, vol. 315, no. 5817, pp. 1416–1420, 2007.
 100. M. A. Ashley-Ross, R. Lundin, and K. L. Johnson, “Kinematics of level terrestrial and underwater walking in the california newt, *taricha torosa*,” *J. of Experimental Zoology Part A: Ecological Genetics and Physiology*, vol. 311, no. 4, pp. 240–257, 2009.
 101. H. Hagihara, S. Wakimoto, T. Kanda, and S. Furukawa, “Operation of a pneumatic soft manipulator using a wearable interface with flexible strain sensors,” in *IROS*. Institute of Electrical and Electronics Engineers Inc., 2019, pp. 4949–4954.
 102. C. Laschi, “Octobot—a robot octopus points the way to soft robotics,” *IEEE Spectrum*, vol. 54, no. 3, pp. 38–43, 2017.
 103. M. Ishida, D. Drotman, B. Shih, M. Hermes, M. Luhar, and M. T. Tolley, “Morphing structure for changing hydrodynamic characteristics of a soft underwater walking robot,” *IEEE RA-L*, vol. 4, no. 4, pp. 4163–4169, 2019.
 104. Q. Hu, E. Dong, G. Cheng, H. Jin, J. Yang, and D. Sun, “Inchworm-inspired soft climbing robot using microspine arrays,” in *IROS*, 2019, pp. 5800–5805.
 105. S. Kim, M. Spenko, S. Trujillo, B. Heyneman, V. Mattoli, and M. R. Cutkosky, “Whole body adhesion: hierarchical, directional and distributed control of adhesive forces for a climbing robot,” in *Proc. IEEE Int. Conf. on Robotics and Automation*, 2007, pp. 1268–1273.
 106. H. E. Jeong, J.-K. Lee, H. N. Kim, S. H. Moon, and K. Y. Suh, “A nontransferring dry adhesive with hierarchical polymer nanohairs,” *Proc. of the National Academy*

- of Sciences*, vol. 106, no. 14, pp. 5639–5644, 2009.
107. T. Hirose, Y. Kakiuchi, K. Okada, and M. Inaba, “Design of soft flexible wire-driven finger mechanism for contact pressure distribution,” in *IROS*, 2019, pp. 4699–4705.
 108. P. H. Nguyen, F. Lopez-Arellano, W. Zhang, and P. Polygerinos, “Design, characterization, and mechanical programming of fabric-reinforced textile actuators for a soft robotic hand,” in *IROS*. Institute of Electrical and Electronics Engineers Inc., 2019, pp. 8312–8317.
 109. C. Jiang, S. A. Nazir, G. Abbasnejad Matikolaie, and J. Seo, “Dynamic flex-and-flip manipulation of deformable linear objects,” 2019.
 110. F. Chen, K. Liu, and X. Zhu, “Buckling-induced shape morphing using dielectric elastomer actuators patterned with spatially-varying electrodes,” in *IROS*, 2019, pp. 8306–8311.
 111. Y.-L. Park, B.-r. Chen, D. Young, L. Stirling, R. J. Wood, E. Goldfield, and R. Nagpal, “Bio-inspired active soft orthotic device for ankle foot pathologies,” in *IROS*, 2011, pp. 4488–4495.
 112. Y.-L. Park, C. Majidi, R. Kramer, P. Bérard, and R. J. Wood, “Hyperelastic pressure sensing with a liquid-embedded elastomer,” *J. of micromechanics and microengineering*, vol. 20, no. 12, p. 125029, 2010.
 113. Y.-L. Park, B.-r. Chen, and R. J. Wood, “Soft artificial skin with multi-modal sensing capability using embedded liquid conductors,” in *SENSORS*, 2011, pp. 81–84.
 114. Y.-L. Park, S. C. Ryu, R. J. Black, K. K. Chau, B. Moslehi, and M. R. Cutkosky, “Exoskeletal force-sensing end-effectors with embedded optical fiber-bragg-grating sensors,” *IEEE TRO*, vol. 25, no. 6, pp. 1319–1331, 2009.
 115. M. Y. Chuah and S. Kim, “Improved normal and shear tactile force sensor performance via least squares artificial neural network (lsann),” in *ICRA*, 2016, pp. 116–122.
 116. J. Rogelio Guadarrama Olvera, E. D. Leon, F. Bergner, and G. Cheng, “Plantar tactile feedback for biped balance and locomotion on unknown terrain,” *Int. J. of Humanoid Robotics*, vol. 17, no. 01, p. 1950036, 2020.



Irene Frizza received her BSc degree in Electronic Engineering from Pisa University in 2016. She received her MSc in Automation and Robotic Engineering from Pisa University in 2019. Currently, she is a PhD candidate with the CNRS-AIST JRL (Joint Robotics Laboratory) at National Institute of Advanced Industrial Science and Technology (AIST), Tsukuba, Japan and with Montpellier University, France. Her research interest includes soft robotic feet, biped locomotion, walking of humanoid robots.



Ko Ayusawa received the B.S. in mechanical engineering, and the M.S. and Ph.D. in mechano-informatics from the University of Tokyo, Japan, in 2006, 2008, and 2011, respectively. He worked with the University of Tokyo, Department of Mechano-Informatics, as a postdoctoral researcher, as a project assistant processor. In 2014, he joined Intelligent Systems Research Institute, National Institute of Advanced Industrial Science and Technology (AIST), Japan. He is currently a senior researcher of Human Augmentation Research Center, AIST, Japan and a senior researcher of CNRS-AIST JRL. His research interests include identification of human/humanoid dynamics, motion control for humanoid robots, and kinematics and dynamics simulation for human musculoskeletal models.



Andrea Cherubini received the MSc in Mechanical Engineering from “Sapienza” University of Rome (2001), the MSc in Control from the University of Sheffield, UK (2003) and the PhD in Control from “Sapienza” (2008). From 2008 to 2011, he was Postdoc at INRIA Rennes, France. Since 2011 he is Associate Professor and since 2021 Full Professor at University of Montpellier, France, where he leads the IDH Group and is in charge of the Robotics Master.



Hiroshi Kaminaga received M.E. from Kyoto University in Mechanical Engineering in 1999. He joined Hewlett-Packard Japan Co. Ltd. in 1999 and ZMP Inc. in 2002. In 2009, he received Ph.D. in Information Science and Technology from The University of Tokyo. JSPS Research Fellow from 2008. Assistant Professor at The University of Tokyo from 2009. Visiting Researcher in DLR (German Aerospace Center) in 2012. He joined Intelligent Systems Research Institute in National Institute of Advanced Industrial Science and Technology (AIST) in 2017 as Senior Researcher. His research interest includes mechatronics system design and control of force sensitive actuators and its applications to humanoid robots.



Philippe Fraise received the master's degree in electrical engineering from the Ecole Normale Supérieure de Cachan, Cachan, France, in 1988, and the Ph.D. degree in automatic control from the University of Montpellier, Montpellier, France, in 1994. He is currently a Professor with the Robotics Department, University of Montpellier. He has authored or co-authored over 150 papers in international peer-reviewed conferences and journals. He was Associate-Editor with IEEE/RAS Transactions on Robotics (2016-2019), Senior Editor with IEEE/RSJ IROS (2018,2019). His research interests include physical human-robot interaction, humanoid robotics, robotics for rehabilitation, and mobile manipulators.



Gentiane Venture received her Engineer's degree from École Centrale de Nantes (France) in 2000, MSc and PhD from University of Nantes (France) in 2000 and 2003 respectively. In 2004 she joined the CEA (France). In 2004 she joined the University of Tokyo (Japan) supported by the JSPS. From 2006 to 2009, she was Project Assistant Professor with the University of Tokyo (Japan). In 2009, she joined Tokyo University of Agriculture and Technology (Japan) as Associate Professor. Since 2016 she is Distinguished Professor and since 2018 cross-appointed fellow with AIST. Her main research interests include: Human body modelling, Control of robot for human/robot interaction. She is presently Senior Editor with RA-L, Associate Editor with TRO, Associate Editor with JRM.